Article

Neuron

Neuroligins Sculpt Cerebellar Purkinje-Cell Circuits by Differential Control of Distinct Classes of Synapses

Highlights

- Purkinje-cell deletion of neuroligins causes loss of distal climbing-fiber synapses
- Cerebellar climbing-fiber synapse numbers depend on all three expressed neuroligins
- Neuroligins KO increases inhibitory synapse size but blocks their function
- Overall, neuroligins are essential for synapse function but not for synaptogenesis

Authors

Bo Zhang, Lulu Y. Chen, Xinran Liu, ..., Sung-Jin Lee, Ozgun Gokce, Thomas C. Südhof

Correspondence

tcs1@stanford.edu

In Brief

Neuroligins are evolutionarily conserved postsynaptic cell-adhesion molecules. Using conditional deletion of neuroligins in cerebellar Purkinje cells, Zhang et al. demonstrate that distinct neuroligin isoforms specify the properties of various Purkinje-cell synapses to shape the overall synaptic responses of Purkinje cells.

Zhang et al., 2015, Neuron *87*, 781–796
August 19, 2015
http://dx.doi.org/10.1016/j.neuron.2015.07.020

CellPress

Neuron
Article

Neuroligins Sculpt Cerebellar Purkinje-Cell Circuits by Differential Control of Distinct Classes of Synapses

Bo Zhang,[1,3] Lulu Y. Chen,[1,3] Xinran Liu,[2] Stephan Maxeiner,[1] Sung-Jin Lee,[1] Ozgun Gokce,[1] and Thomas C. Südhof[1,*]
[1]Department of Molecular and Cellular Physiology and Howard Hughes Medical Institute, Stanford University Medical School, 265 Campus Drive, Room G1021, Stanford, CA 94305, USA
[2]Department of Cell Biology, Yale University School of Medicine, New Haven, CT 06510, USA
[3]Co-first author
*Correspondence: tcs1@stanford.edu
http://dx.doi.org/10.1016/j.neuron.2015.07.020

SUMMARY

Neuroligins are postsynaptic cell-adhesion molecules that bind presynaptic neurexins and are genetically linked to autism. Neuroligins are proposed to organize synaptogenesis and/or synaptic transmission, but no systematic analysis of neuroligins in a defined circuit is available. Here, we show that conditional deletion of all neuroligins in cerebellar Purkinje cells caused loss of distal climbing-fiber synapses and weakened climbing-fiber but not parallel-fiber synapses, consistent with alternative use of neuroligins and cerebellins as neurexin ligands for the excitatory climbing-fiber versus parallel-fiber synapses. Moreover, deletion of neuroligins increased the size of inhibitory basket/stellate-cell synapses but simultaneously severely impaired their function. Multiple neuroligin isoforms differentially contributed to climbing-fiber and basket/stellate-cell synapse functions, such that inhibitory synapse-specific neuroligin-2 was unexpectedly essential for maintaining normal climbing-fiber synapse numbers. Using systematic analyses of all neuroligins in a defined neural circuit, our data thus show that neuroligins differentially contribute to various Purkinje-cell synapses in the cerebellum in vivo.

INTRODUCTION

Neuroligins are cell-adhesion molecules that were identified as postsynaptic ligands for presynaptic neurexins (Ichtchenko et al., 1995). Mammals co-express four neuroligins (neuroligin-1 to -4, referred to as NL1 to NL4; Ichtchenko et al., 1996; Bolliger et al., 2008) that are localized to subsets of synapses. NL1 is targeted to glutamatergic synapses, NL2 is found in GABAergic and cholinergic synapses, NL3 is present in both glutamatergic and GABAergic synapses, and NL4 is detected in glycinergic synapses but may also function in excitatory synapses (Song et al., 1999; Varoqueaux et al., 2004; Budreck and Scheiffele, 2007; Zhang et al., 2009; Hoon et al., 2011; Takács et al., 2013). NL1, NL2, and NL3 are highly conserved throughout evolution, whereas NL4 diverges significantly even between rodents and primates (Bolliger et al., 2008). Neuroligins constitutively homodimerize in a *cis* configuration, and NL1 and NL3 may also heterodimerize (Araç et al., 2007; Chen et al., 2008; Fabrichny et al., 2007; Poulopoulos et al., 2012). Neuroligins bind to neurexins in a *trans*-configuration to form an intercellular junction (Nguyen and Südhof, 1997) and also interact with other *cis*- and *trans*-ligands (Ko et al., 2009a, 2009b; Lee et al., 2013; Pettem et al., 2013). Preliminary analyses suggest that different neuroligin-neurexin combinations exhibit distinct binding affinities depending on the precise isoforms and splice variants involved (Boucard et al., 2005; Chih et al., 2006; Comoletti et al., 2006; Araç et al., 2007), although no systematic comparisons have been performed.

Human neuroligin gene mutations appear to cause autism and/or intellectual disability with nearly 100% penetrance, usually as de novo mutations arising in the germline (reviewed in Chen et al., 2014; Südhof, 2008). Multiple rare missense and deletion mutations in human *NLGN1*, *NLGN3*, and *NLGN4* genes have been described (for early papers, see Jamain et al., 2003; Laumonnier et al., 2004; Yan et al., 2005). Most disease-associated neuroligin mutations are probably pathogenic by a loss-of-function mechanism, but some neuroligin mutations may mediate gain-of-function effects, as documented for the R451C substitution in *NLGN3* (Tabuchi et al., 2007; Etherton et al., 2011; Földy et al., 2013).

Despite their importance, considerable uncertainty surrounds the functions of neuroligins. Hundreds of papers using diverse approaches have yielded different, often contradictory conclusions. In mice, constitutive triple knockout (KO) of NL1, NL2, and NL3 produced lethality, probably because of impairments in synaptic transmission (Varoqueaux et al., 2006), while constitutive single KOs of individual neuroligins caused robust non-lethal synaptic phenotypes (Chubykin et al., 2007; Jamain et al., 2008; Gibson et al., 2009; Poulopoulos et al., 2009; Etherton et al., 2011; Baudouin et al., 2012; Jedlicka et al., 2013). Neither single nor triple constitutive neuroligin KO mice exhibited a decrease in synapse numbers. In contrast, RNAi-dependent "knockdown" experiments of individual neuroligins revealed a massive loss of synapses in vitro and in vivo (Chih et al., 2005; Kwon et al., 2012).

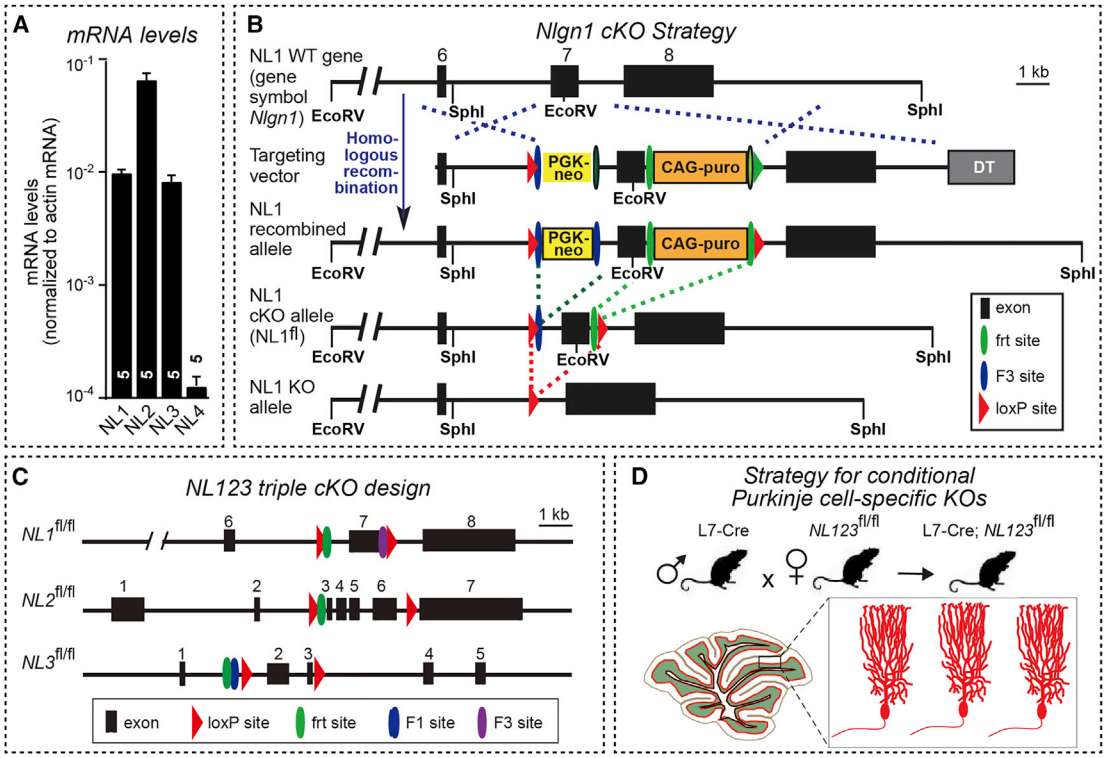

Figure 1. Generation of Purkinje Cell-Specific Neuroligin-1/2/3 Conditional KO Mice

(A) Quantitative RT-PCR shows that NL1, NL2, and NL3 are abundantly expressed in cerebellum, whereas NL4 is undetectable. Levels of mRNA are shown as percentage of actin mRNA levels (means ± SEM; n = 5 mice).

(B and C) Strategy for generation of NL1 cKO mice (B) and comparison of the design of all three neuroligin cKO alleles (C). Exon numbers are indicated above the boxes.

(D) Breeding strategy for generation of Purkinje cell-specific neuroligin cKO mice using L7-cre transgenic mice.

For additional data, see Figures S1–S3.

Electrophysiologically, NL1 KOs and knockdowns in hippocampal neurons induced a decrease in synaptic responses mediated by NMDA receptors (NMDARs) but not by AMPA receptors (AMPARs; Chubykin et al., 2007; Kim et al., 2008; Blundell et al., 2010; Kwon et al., 2012; Soler-Llavina et al., 2011; Shipman and Nicoll, 2012). In contrast, NL2 and NL3 KOs caused selective impairments in subsets of GABAergic synapses (Chubykin et al., 2007; Gibson et al., 2009; Poulopoulos et al., 2009; Etherton et al., 2011; Földy et al., 2013; Rothwell et al., 2014). Overexpression of all neuroligin isoforms, conversely, increased synapse numbers as assessed morphologically (Boucard et al., 2005; Chih et al., 2005; Ko et al., 2009b; Sara et al., 2005; Zhang et al., 2009). In addition, overexpression of NL1 enhanced both NMDAR- and AMPAR-mediated excitatory postsynaptic currents (EPSCs), overexpression of NL2 selectively increased inhibitory postsynaptic currents (IPSCs), and overexpression of NL4 paradoxically decreased NMDAR- and AMPAR-mediated EPSCs, whereas overexpression of NL3 produced no electrophysiological effect (Chubykin et al., 2007; Ko et al., 2009b; Zhang et al., 2009; Chanda et al., 2013).

Thus, constitutive KOs and acute knockdowns of neuroligins have very different phenotypes in neurons, neuroligin loss-of-function and overexpression experiments do not cause complementary effects, and synapses induced by neuroligin overexpression are often likely non-functional. The divergence between these results may derive from difficulties in interpreting some of the experimental approaches used. Constitutive KOs of neuroligins may elicit developmental compensation that could obscure important functions. Conversely, knockdowns (that are invariably based on micro-RNA biology both with shRNAs and the micro-RNA method) may produce off-target effects and inherently cause disruptions of endogenous micro-RNA-based processes that normally regulate neurons. Finally, a neuroligin isoform may have multiple, parallel functions but only a subset of these functions may be redundant among isoforms, thereby preventing recognition of these redundant functions.

In an attempt to help clarify some of these central issues, we have chosen here a systematic approach and analyzed the effects of single, double, and triple conditional KOs (cKOs) of neuroligins in a well-defined neural circuit, the cerebellar Purkinje-cell circuit that has been implicated in ASD pathogenesis (Wang et al., 2014). In mouse cerebellum, NL4 is not detectably expressed (Figure 1A), allowing us to focus on NL1, NL2, and NL3. We generated cKO mice for NL1 and used previously generated cKOs of NL2 and NL3 (Rothwell et al., 2014;

Liang et al., 2015) to morphologically and electrophysiologically analyze the functions of all three neuroligins in cerebellum. Our study represents an initial systematic analysis of all neuroligins expressed in a specific circuit, constitutes the first examination of multiple cKOs for neuroligins in the same type of neuron, and allows a direct comparison of the relative contributions of different neuroligins to distinct synapses. Our data reveal that neuroligins differentially contribute to different synapses in an interactive manner and that their function enables synaptic transmission but is not essential for synapse formation.

RESULTS

Generation of Purkinje Cell-Specific Single, Double, and Triple Neuroligin cKO Mice

Measurements of total neuroligin mRNA levels in mouse cerebellum by quantitative RT-PCR revealed that NL1, NL2, and NL3 were abundantly expressed, with NL2 exhibiting highest levels (Figure 1A). NL4 mRNAs, however, were present at extremely low levels, prompting us to focus on NL1, NL2, and NL3.

We generated NL1 cKO mice using standard approaches that were rendered difficult by a low homologous recombination rate, which necessitated the use of two selectable markers in the targeting vector (Figure 1B). After validation, we crossed NL1 cKO mice with previously obtained NL2 and NL3 cKO mice (Rothwell et al., 2014; Liang et al., 2015) to produce double NL1 and NL3 (NL13), double NL2 and NL3 (NL23), and triple NL1, NL2, and NL3 (NL123) cKO mice (Figure 1C). We then crossed the single, double, and triple neuroligin cKO mice with L7-Cre mice that express Cre-recombinase under control of the Purkinje cell-specific L7 promoter (Figures 1D and S1; Barski et al., 2000).

Triple NL123-KO mice harboring the L7-Cre transgene did not exhibit premature mortality at 4 months of age (n = 41/38 littermate control/L7-Cre NL123-KO mice), had a normal body weight, and displayed no obvious anatomical abnormalities (Figure S1). Immunoblotting of cerebellar proteins from adult triple Purkinje cell-specific NL123-KO mice revealed decreases in NL1, NL2, and NL3 proteins of ~40%, ~30%, and ~40%, respectively (Figure S2); similar reductions of neuroligins were also observed in single and double Purkinje cell-specific neuroligin KO mice (Figure S3). Since Purkinje cells account for a minority of cerebellar neurons, this result suggests that Purkinje cells abundantly express NL1, NL2, and NL3. Besides neuroligins, the only other proteins examined that exhibited expression changes in NL123-KO mice were PICK1 (~30% decrease) and α-neurexins (~30% decrease). In particular, mGluR1/5 levels were unaltered. Since this result contrasts a previous report on constitutive NL3 KO mice (Baudouin et al., 2012), we reanalyzed the constitutive NL3 KO mice with two different antibodies but again detected no change in mGluR1/5 levels (Figure S2).

Viewed together, these data suggest that deletion of neuroligins from cerebellar Purkinje cells does not significantly alter mouse survival, mouse welfare, and cerebellar development.

Purkinje Cell-Specific Triple NL123-KO Differentially Alters Cerebellar Synapse Numbers and Sizes

We stained cerebellar sections from littermate control and NL123-KO mice with antibodies to vGluT1 and vGluT2 to specifically label parallel-fiber and climbing-fiber synapses, respectively (Lorenzetto et al., 2009). We observed a dramatic decrease (~50%) in the density of climbing-fiber synapses (vGluT2 puncta) on distal Purkinje-cell dendrites but only a modest decrease (~15%) in climbing-fiber synapse density on proximal dendrites (Figures 2A and 2B). Moreover, we detected a uniform decrease (~25%) in the size of climbing-fiber synapses on both distal and proximal Purkinje cell dendrites (Figure 2B). In contrast to vGluT2-containing climbing-fiber synapses, individual puncta of vGluT1-containing parallel-fiber synapses could not be resolved owing to their high density. Therefore, we quantified the total vGluT1 immunofluorescence intensity as a measure of parallel-fiber synapse density and validated this approach using cerebellin-1 KO mice, which are known to exhibit a decrease in parallel fiber synapses (Figure S1D; Hirai et al., 2005). We detected no difference in cerebellar vGluT1 signal between littermate control and NL123-KO mice, suggesting that parallel-fiber synapses were not altered (Figures 2A and 2B).

We next analyzed inhibitory inputs onto Purkinje cells. Surprisingly, staining of cerebellar cortex for the vesicular GABA transporter (vGAT) as a marker of GABAergic presynaptic terminals revealed that the Purkinje cell-specific NL123-KO caused a significant increase in inhibitory synapse size without affecting synapse numbers (Figures 2C and 2D). Staining with another GABAergic synapse maker, GAD65, also revealed an increase in inhibitory synapse size in NL123-KO mice but also detected an increase in puncta density, probably as an indirect consequence of the increased synapse size (Figures S4A and S4B).

To confirm the light microscopy observations, we performed electron microscopy (EM) analyses of cerebellar synapses (Figures 2D–2F). Consistent with the light microscopy results, the bouton size of climbing-fiber synapses was reduced in Purkinje cell-specific NL123-KO mice, whereas the PSD95 length and vesicle density in parallel-fiber synapses was normal and parallel-fiber synapse density was unchanged. In contrast, basket cell/stellate cell synapses onto Purkinje cells were increased in size (Figures 2D and 2E). Thus, the EM data validate the immunocytochemistry results.

Triple Neuroligin cKO in Purkinje Cells Impairs Climbing but Not Parallel-Fiber Synapse Function

We performed whole-cell patch-clamp recordings in acute cerebellar slices from juvenile (postnatal days 21–25 [P21–P25]) littermate control and Purkinje cell-specific NL123-KO mice (Figure 3A). We detected an ~40% decrease in the amplitude of climbing-fiber excitatory postsynaptic currents (EPSCs) in mutant mice (Figure 3B) but observed no changes in the kinetics (rise and decay times) or paired-pulse ratio (PPR) of EPSCs (Figures 3C and 3D). Adult Purkinje cell-specific NL123-KO mice (~P63) exhibited similar reductions in the climbing-fiber synapse EPSC amplitude (Figures 3B and S3C). Climbing-fiber synapse elimination was normal in young and adult Purkinje cell-specific NL123-KO mice as evidenced by single-step climbing-fiber synaptic responses (Figures 3E and S4D).

To determine whether the decreased climbing-fiber synapse EPSCs resulted from a reduction of functional release sites or a decrease in quantal size, we measured Sr^{2+}-mediated delayed quantal release events that trail evoked climbing-fiber synapse

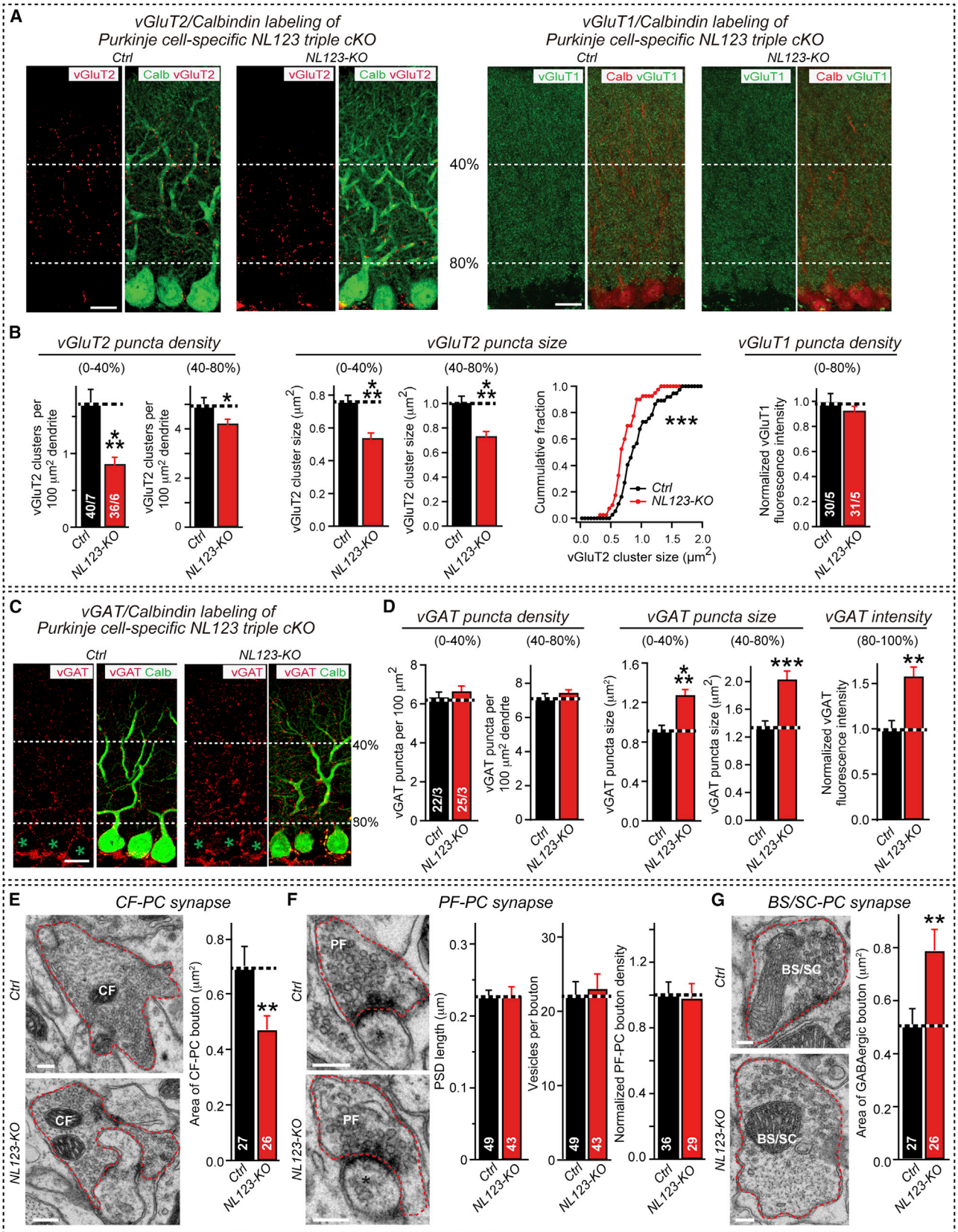

(legend on next page)

EPSCs (Xu-Friedman and Regehr, 2000). We found a significant decrease in the frequency of delayed quantal release events per trial in Purkinje cell-specific NL123-KO mice, but not in the amplitude of events (Figure 3F), consistent with an impairment in synapse function.

We next analyzed EPSCs mediated by parallel-fiber synapses, the other excitatory synaptic input onto Purkinje cells, but detected no changes. Specifically, we observed in Purkinje cell-specific NL123-KO mice no alterations in the input-output curve, the PPR, or the kinetics of parallel-fiber synapse EPSCs (Figures 3G, 3H, and S4D). Moreover, we found no change in DHPG-triggered long-term depression (LTD) in neuroligin-deficient Purkinje cells (Figure 3I). Since the latter result was surprising given a previous report that constitutive NL3 KO mice exhibit a loss of DHGP-induced LTD (Baudouin et al., 2012), we also measured DHPG-induced LTD in constitutive NL3 KO mice. Again, we observed no impairment (Figure S4G). Finally, we detected in Purkinje cell-specific NL123-KO mice no changes in the frequency or amplitude of Purkinje cell mEPSCs, which are derived primarily from parallel-fiber synapses (Figure 3J). Combined with the vGluT1 staining and EM results (Figures 2A, 2B, and 2E), these data suggest that parallel-fiber synapses are normal in Purkinje cells lacking neuroligins.

Triple Neuroligin cKO in Purkinje Cells Severely Impairs Inhibitory Synaptic Transmission

We recorded inhibitory postsynaptic currents (IPSCs) from Purkinje cells in response to extracellular stimulation. In these recordings, we placed the stimulus electrodes close to the patched Purkinje cell. Thereby, we preferentially monitored IPSCs from basket-cell synapses that are formed on proximal dendrites and the soma of Purkinje cells (Figure 3A).

We observed a large (~80%) decrease in IPSC amplitude in Purkinje cells lacking neuroligins, without major changes in IPSC kinetics (Figure 4A). We detected no alteration in paired-pulse ratio (PPR), suggesting that the decrease in IPSC amplitude is caused by a postsynaptic change.

We then monitored spontaneous miniature IPSCs (mIPSCs) that are likely derived from both proximal basket cell synapses and distal stellate cell synapses. We detected a large decrease in mIPSC frequency (~80%) and amplitude (~45%), indicating impaired inhibitory synapse function in both basket- and stellate-cell synapses (Figures 4B and S3D). We also observed a decrease in the decay but not rise times of mIPSCs, possibly suggesting that the remaining mIPSCs were largely from proximal dendrosomatic synapses that tend to exhibit faster decay times (Spruston et al., 1994). Importantly, we found that IPSCs induced by direct puffing of GABA onto Purkinje cells were indistinguishable between control and NL123-KO neurons (Figure 4C) and that the density of interneurons in the cerebellum of NL123-KO mice was normal (Figure S4F). Thus, the NL123-KO has no effect on the surface transport of GABA receptors or inhibitory synapse formation on Purkinje cells but selectively impairs synaptic transmission at GABAergic synapses by decreasing the GABA-receptor content of these synapses.

Conditional Acute Neuroligin Deletion in Juvenile Mice Recapitulates Phenotype Induced by NL123-KO throughout Development

A critical issue with constitutive KOs is the potential for developmental compensation. The NL123-KO used here does not address this issue because deletion of neuroligins was driven by L7-Cre expression, which initiates during development, albeit late. To test whether developmental compensation may have occluded a more severe NL123-KO phenotype that could develop upon acute deletions of neuroligins in mature neurons, we stereotactically injected AAVs expressing EGFP-tagged mutant inactive (ΔCre) or wild-type active Cre-recombinase (Cre) into the cerebellum of NL123 cKO mice at P21. We then cut acute slices from the cerebellum at P35 (Figure 5A) and analyzed key features of the NL123-KO phenotype electrophysiologically (Figures 5B and 5C). We observed the same robust reduction in the climbing-fiber synapse EPSC amplitude and a similar decrease in both the frequency and amplitude of basket/stellate cell mIPSCs after acute deletion of neuroligins in Purkinje cells as in L7-cre NL123-KO mice, suggesting that these parameters were not subject to developmental compensation.

Viewed together, the data up to now indicate that the deletion of all neuroligins from Purkinje cells has dramatically different effects on their three principal synapse types: climbing-fiber synapses are selectively reduced in numbers on peripheral Purkinje cell dendrites and exhibit a decrease in synaptic

Figure 2. Purkinje Cell-Specific NL123-KO Decreases the Size and Territory of Climbing-Fiber Synapses but Increases the Size of Inhibitory Basket/Stellate Cell Synapses

(A) Representative confocal images of cerebellar sections from littermate control (Ctrl) and Purkinje cell-specific NL123-KO mice. Sections were double labeled for calbindin (green, to label Purkinje cells) and vGluT2 or vGluT1 (red, to visualize climbing- and parallel-fiber synapses, respectively; scale bars = 20 μm).

(B) NL123-KO decreases climbing-fiber synapses on distal Purkinje cell dendrites and reduces climbing-fiber synapse size throughout all Purkinje cell dendrites but does not alter parallel-fiber synapses as quantified via vGluT2 and vGluT1 signals, respectively. Note that parallel-fiber synapses could not be individually quantified because of high synapse density (A, right); instead, we measured the overall vGluT1 immunofluorescence signal which reflects parallel-fiber synapse numbers (Figure S1D).

(C) Representative confocal images of cerebellar sections double labeled for vGAT (red, to visualize inhibitory synapses) and calbindin (green; scale bars = 20 μm).

(D) NL123-KO increases inhibitory synapse size as quantified via vGAT staining without affecting inhibitory synapse density.

(E–G) Electron microscopy shows that the NL123-KO decreases climbing-fiber synapse size, increases inhibitory synapse size, and leaves parallel-fiber synapse morphology and density unchanged. Panels show representative EM images (left) and summary graphs (right) of the presynaptic area of climbing-fiber synapses (E), the PSD length, vesicle numbers per bouton, and synapse density of parallel-fiber synapses (F), and of the presynaptic area of inhibitory stellate/basket cell synapses (G). Scale bars = 0.2 μm.

Data are represented as means ± SEM; statistical analyses were performed by two-tailed Student's t test (bar diagrams) or Kolmogorov-Smirnov test (cumulative distributions); *$p < 0.05$, **$p < 0.01$, and ***$p < 0.001$. Numbers of sections/mice analyzed are shown in bar graphs for (B) and (D); numbers of synapses analyzed from two mice per genotype are listed in bar graphs for (E)–(G).

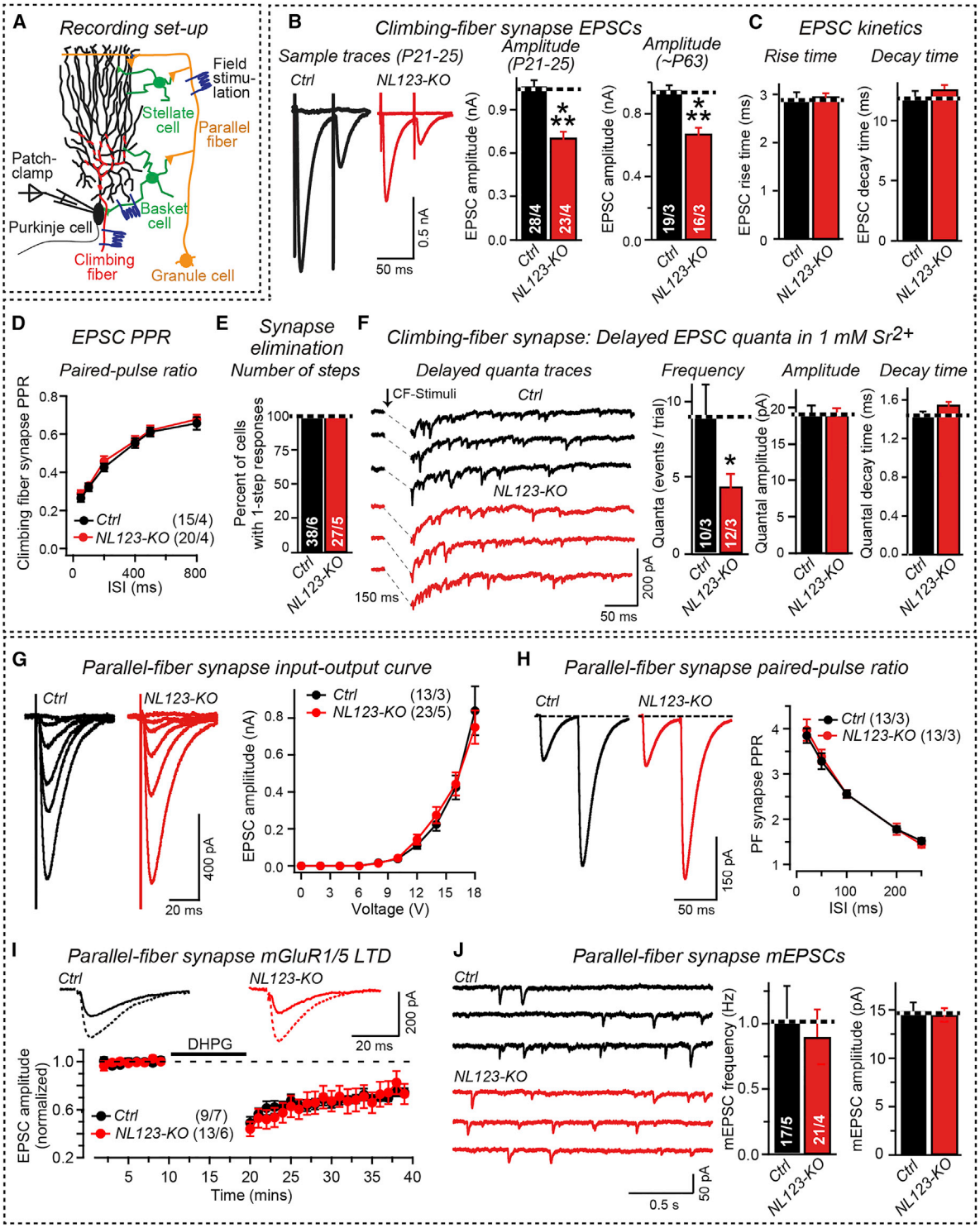

Figure 3. Purkinje Cell-Specific Conditional NL123-KO Impairs Climbing-Fiber but Not Parallel-Fiber Synaptic Transmission

(A) Diagram of the recording configuration.

(B) Representative traces of climbing-fiber EPSCs elicited in acute cerebellar slices by two stimuli with 50 ms interval (left) and summary graphs of the EPSC amplitude from littermate control (Ctrl) and Purkinje cell-specific NL123-KO mice at P21–P25 (middle) and at P60–P65 (right).

(C) Summary graphs of climbing-fiber EPSC kinetics recorded as in (B) at P21–P25.

(D) Normal paired-pulse ratios (PPRs) of climbing-fiber synapses in Purkinje cell-specific NL123-KO mice at P21–P25.

(legend continued on next page)

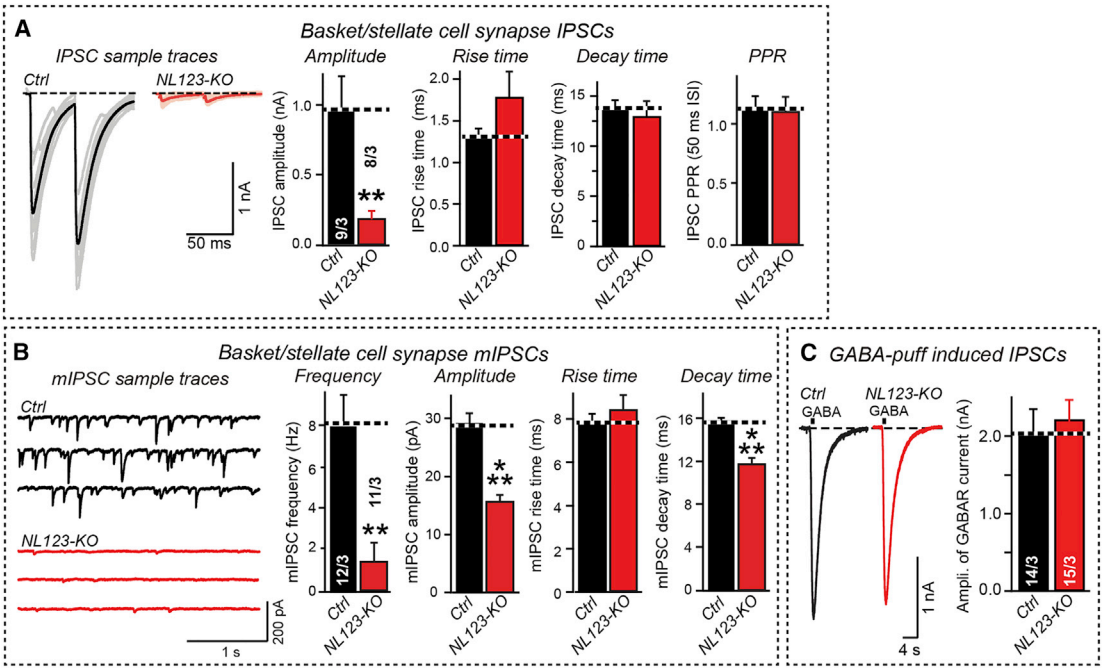

Figure 4. Purkinje Cell-Specific Conditional NL123-KO Severely Impairs Inhibitory Synapse Function

(A) NL123-KO decreases the IPSC amplitude without changing the PPR or IPSC kinetics. Panels depict representative IPSC traces (left) and summary graphs of the IPSC amplitude (middle left), kinetics (middle), and PPRs (right) in control and Purkinje cell-specific NL123-KO mice.

(B) NL123-KO impairs the amplitude, frequency, and decay kinetics of spontaneous mIPSCs monitored in 1 μM TTX. Panels show representative traces (left) and summary graphs of the mIPSC frequency and amplitude (left two plots) and of the mIPSC kinetics (right two plots).

(C) NL123-KO has no effect on GABAR-mediated IPSCs induced by local puffing of GABA (50 μM, injected at 8 psi for 1 s) onto Purkinje cells (left, representative traces; right, summary graphs).

All data are represented as means ± SEM; numbers of neurons/mice analyzed are shown in the bars or plots. Inter-group comparisons were done by two-tailed Student's t test (**p < 0.01, ***p < 0.001). For additional data, see Figure S3.

strength; parallel-fiber synapses are unaffected consistent with a role for cerebellins as neurexin ligands in these synapses (Matsuda et al., 2010; Uemura et al., 2010); and inhibitory basket/stellate cell synapses are increased in size but functionally inactivated, effectively producing not "silent" but "deaf-mute" inhibitory synapses. These results raise the possibility of a "neuroligin code" whereby neuroligins are not essential for synapse formation or synapse maintenance as such but differentially contribute to the operability of specific types of synapses in a given neuronal circuit.

Deconstructing Climbing-Fiber Synapse Functions of Individual Neuroligins

To determine the contributions of various neuroligin isoforms to the climbing-fiber synapse phenotype in Purkinje cell-specific NL123-KO mice, we first examined Purkinje cell-specific double NL13-KO mice. Surprisingly, the NL13-KO did not cause a loss of distal climbing-fiber synapses as assessed by vGluT2 staining but produced only a small uniform loss (~5%) of synapse numbers (Figures 6A and 6B). However, the NL13-KO induced the same decrease in synapse size as the triple NL123-KO

(E) Normal climbing-fiber synapse elimination in Purkinje cell-specific NL123-KO mice. Summary graph depicts percentage of neurons exhibiting a single-step EPSC response after application of increasingly strong above-threshold stimuli.

(F) Analysis using Sr^{2+} reveals that the frequency of quantal climbing-fiber synaptic events in NL123-KO Purkinje cells is decreased ~2-fold (left, representative traces of the decay phase of EPSCs monitored in 1 mM Sr^{2+}/0 mM Ca^{2+}/2 mM Mg^{2+}; right, summary graphs of the quantal event frequency, amplitude, and decay kinetics).

(G) Input/output relation of parallel-fiber synapses in control and NL123-KO Purkinje cells (left, representative traces; right, summary plot).

(H) Normal PPRs as measured in parallel-fiber synapses at increasing inter-stimulus intervals in control and NL123-KO Purkinje cells (left, representative traces; right, summary plot).

(I) mGluR1/5-dependent LTD is normal in NL123-KO parallel-fiber synapses (top, representative traces; bottom, summary plot). For normal LTD in constitutive NL3 KO mice, see Figure S4G.

(J) Analysis of spontaneous mEPSCs (which are largely derived from parallel-fiber synapses) monitored in 1 μM TTX in control and NL123-KO Purkinje cells (left, representative traces; right, summary plots of the mESPC frequency and amplitude).

All data are represented as means ± SEM; numbers of neurons/mice analyzed are shown in the bars or plots. Inter-group comparisons were done by two-tailed Student's t test; multiple comparisons were analyzed with one-way ANOVA with Bonferroni's post-test (*p < 0.05, ***p < 0.001). For additional data, see Figures S4 and S5.

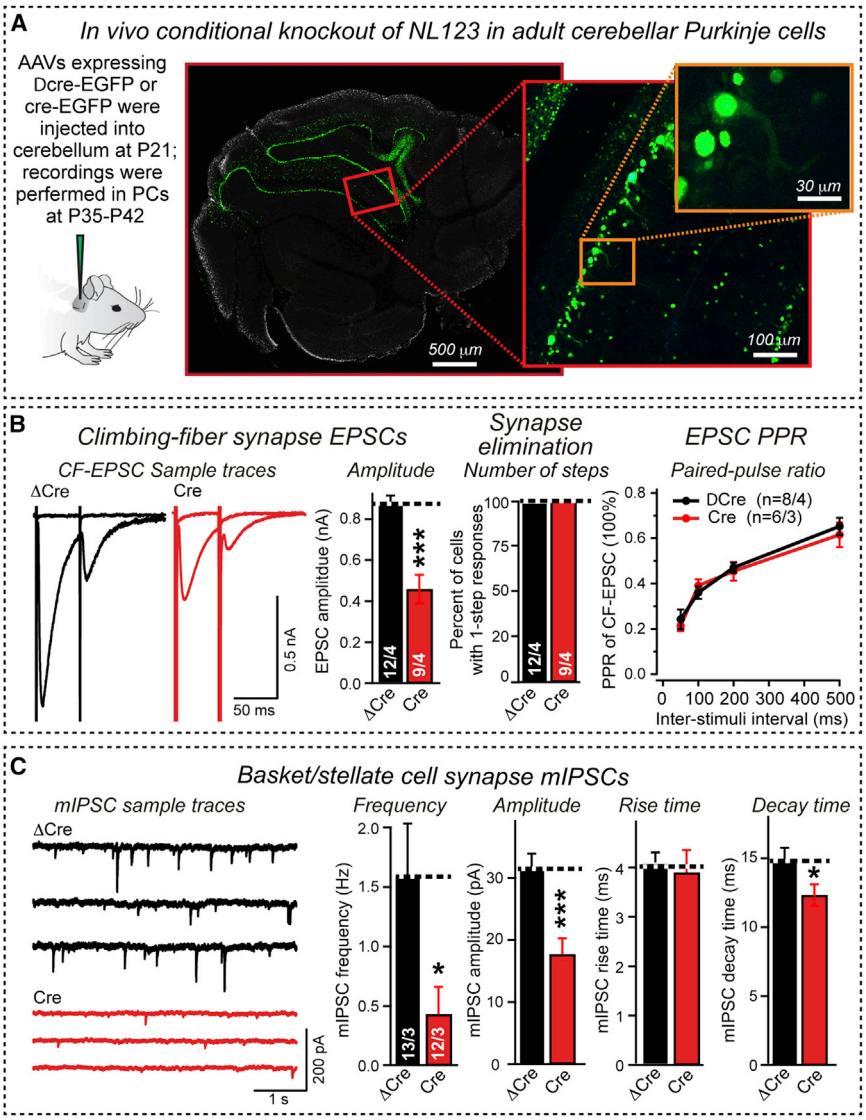

Figure 5. Acute Conditional NL123-KO by Stereotactic Injection of AAVs Expressing Wild-Type Cre-Recombinase Replicates the NL123-KO Phenotype Induced by Transgenic Cre-Recombinase Expression

(A) Experimental strategy. Left, stereotactic injection approach; center and right, representative fluorescence images of Purkinje cells in cerebellar slices cut at P35 from mice that had been stereotactically injected at P21 with AAVs expressing EGFP-tagged Cre or ΔCre.

(B) Virally induced conditional NL123-KO in Purkinje cells reproduces the climbing-fiber synapse phenotype observed after transgenic deletion of neuroligins (left, representative EPSCs and summary graphs of EPSC amplitudes; center, synapse elimination; right, PPRs).

(C) Virally induced conditional NL123-KO in Purkinje cells reproduces the inhibitory synapse phenotype observed after transgenic deletion of neuroligins (left, representative traces; right, summary graphs of mIPSC amplitude, frequency, rise time, and decay time).

Data shown in summary graphs are represented as means ± SEM; inter-group comparisons were done by two-tailed Student's t test. For multiple comparisons data were analyzed with one-way ANOVA with Bonferroni's post-test. (*$p < 0.05$ and ***$p < 0.001$).

(~25%; compare Figures 2B versus 6B). Thus, the apparent size of climbing-fiber synapses was dependent only on NL1 and NL3, which are known to be present in excitatory synapses, whereas the number of climbing-fiber synapses was "normalized" in NL13-KO mice by the continued expression of NL2, which is paradoxically known to be specific for inhibitory synapses (Varoqueaux et al., 2004).

We next measured the effect of the double NL13-KO on climbing-fiber synapse EPSCs but detected only a modest decrease in EPSC amplitude (~10%), with no change in PPR or synapse elimination (Figures 6C, S5A, and S5B). Examination of single NL1- or NL3-KO mice revealed that each single cKO produced a similar small decrease in climbing-fiber synapse EPSC amplitude comparable to that of the double NL13-KO (Figures 6D and 6E). Neither manipulation dramatically changed the PPR (Figures S5D and S5E). Like NL123-KO mice, moreover, Purkinje cell-specific NL13-, NL1-, or NL3-KO mice exhibited no change in parallel-fiber synaptic transmission (Figures 6F, 6G, and S5F). Finally, basket/stellate-cell synapse-mediated mIPSCs displayed no changes in any of those KOs (Figures 6H, S5C, and S5G).

Thus, NL1 and NL3 make essential contributions to organizing climbing-fiber synapses, but the remaining expression of NL2 in NL13-KO mice is sufficient to maintain normal climbing-fiber synapse numbers. NL2 therefore not only contributes to enabling inhibitory synapse function, but also to maintaining excitatory climbing-fiber synapse numbers.

Purkinje Cell-Specific Double NL23-KO and Single NL2-KO Severely Impair Inhibitory Synaptic Transmission without Altering Inhibitory Synapse Numbers

vGluT2 staining and climbing-fiber synapse recordings in NL23-KO mice revealed a slight reduction in vGluT2 cluster density and size and a decrease in climbing-fiber EPSC amplitude without a change in climbing-fiber quantal events as measured in Sr^{2+} (Figures 7A–7C and S6A). Again, no abnormalities in parallel-fiber synaptic transmission were noted (Figures 7D and 7E). Measurements of mIPSCs in NL23-KO mice, however, uncovered a large decrease in both the frequency (~90%) and amplitude (~45%) of mIPSCs (Figures 7F and S6B), similar to the phenotype of triple NL123-KO mice (Figure 4).

To estimate how much of the triple NL123-KO and the double NL23-KO phenotype was exclusively due to the deletion of NL2

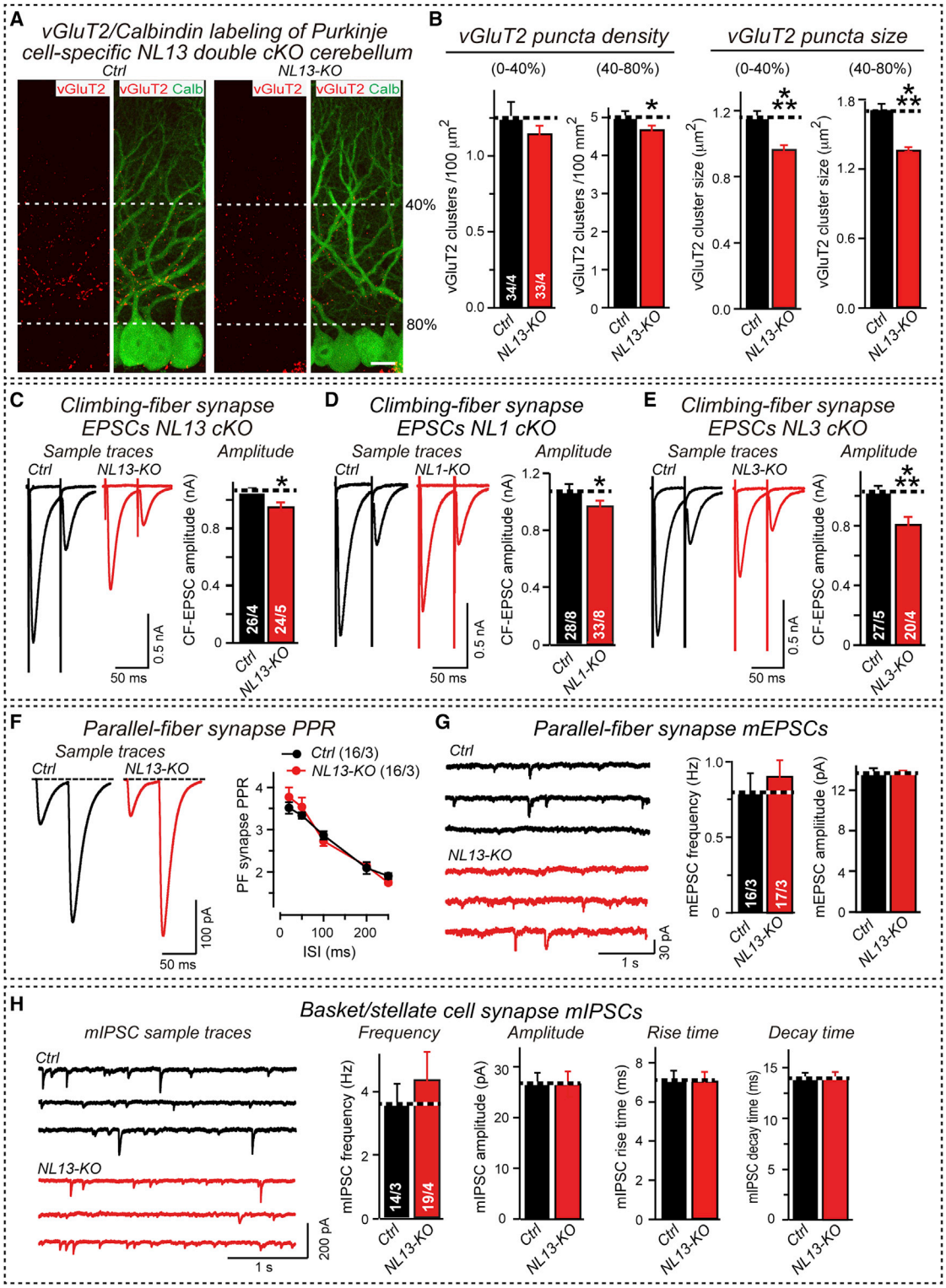

Figure 6. Both NL1 and NL3 Contribute to Climbing-Fiber Synapse Function

(A) Representative confocal images of cerebellar sections double labeled for calbindin (green, to label Purkinje cells) and vGluT2 (red, to visualize climbing-fiber synapses). Sections were from littermate control (Ctrl) and Purkinje cell-specific double NL13-KO mice (scale bar = 20 µm).

(B) Climbing-fiber synapse density (left), as assessed by vGluT2 staining, is marginally impaired by the double NL13-KO, whereas climbing-fiber synapse size (right) is uniformly decreased.

(legend continued on next page)

as the prototypical inhibitory synapse-specific neuroligin, we examined Purkinje cell-specific NL2-KO mice. We observed no significant change in the density, distribution, or size of excitatory climbing-fiber synapses labeled with antibodies to vGluT2 or of inhibitory basket/stellate cell synapses labeled with antibodies to GAD65 (Figures 8A–8D). Thus, the NL2-KO alone does not cause the loss of distal climbing-fiber synapses that is present in triple NL123-KO cerebellum but not in double NL13-KO cerebellum (Figures 2A, 2B, 6A, and 6B). Moreover, the NL2-KO alone also does not produce the increase in inhibitory synapse size that is observed in triple NL123-KO cerebellum (Figures 2C and 2D).

We then examined synaptic function in Purkinje cell-specific NL2-KO mice. Surprisingly, we observed an ~25% increase in the climbing-fiber synapse EPSC amplitude but an ~50% reduction in the IPSC amplitude; neither EPSCs nor IPSCs exhibited a change in PPR (Figures 8E, 8F, and S6C). Moreover, the spontaneous mIPSC frequency was decreased ~67% in NL2-deficient Purkinje cells without a change in mIPSC amplitude or kinetics (Figure 8G). Thus, the single NL2-KO in Purkinje cells causes a loss of inhibitory synaptic strength without an alteration in synapse numbers or size, synaptic release probability, or mIPSC amplitude. As a result, the dissociation of inhibitory phenotypes is striking: the NL3-KO has no phenotype, the NL2-KO produces a decrease in mIPSC frequency but not amplitude, whereas the double NL23-KO causes dramatic decreases both in mIPSC frequency and amplitude.

DISCUSSION

In a systematic analysis, we determined the overall role of neuroligins in all synapses of Purkinje cells, which are the only output neurons of the cerebellar cortex (Ito, 2002), and deconvolved the shared and distinct roles of different neuroligins in sculpting cerebellar Purkinje-cell circuits. Our data provide insight into the general functions of neuroligins and identify differential contributions of different neuroligins to the organization of distinct cerebellar synapses (Figure S8).

The Overall Functions of Neuroligins

We would like to propose three general conclusions about neuroligins based on our data. First, neuroligins are not required for synapse formation as such. In excitatory climbing-fiber synapses, deletion of neuroligins caused a loss of only distal synapses that account for a minor percentage of the total synapses (Figure 2). In inhibitory basket/stellate cell synapses, deletion of neuroligins did not change synapse numbers but increased their size (Figure 2), even though it nearly silenced their function (Figure 4).

Second, neuroligins are selectively important for postsynaptic functions. We detected no biologically significant changes in the PPR of EPSCs and IPSCs or in EPSC and IPSC kinetics under any condition. We observed a decrease in mini frequency for inhibitory synapses and in the frequency of delayed unitary Sr^{2+}-triggered events for climbing-fiber synapses, suggesting that in the absence of neuroligins, a subset of synapses are rendered ''deaf'' (used to characterize a state of unresponsiveness as opposed to excitatory ''silent'' synapses in which AMPA-receptor responses are selectively lost). This finding corroborates previous conclusions that neuroligins function primarily as synaptic organizers (Varoqueaux et al., 2006; Chubykin et al., 2007).

Third, different neuroligins differentially contribute to distinct synapses. Although there was redundancy (e.g., between NL2 and NL3 in inhibitory synapses), each neuroligin isoform provided a unique contribution. Moreover, despite synapse specificity of NL2 for inhibitory synapses, NL2 indirectly shaped the properties of excitatory synapses. Thus, even NL1 and NL3, which are both targeted to excitatory synapses, and NL2 and NL3, which are both targeted to inhibitory synapses, perform distinct functions.

Distinct Roles of Neuroligins in Different Cerebellar Synapses

We find that neuroligins have no detectable role in parallel-fiber synapses, presumably because presynaptic parallel fibers secrete cerebellins that connect presynaptic neurexins with postsynaptic GluRδ2 receptors (Matsuda et al., 2010; Uemura et al., 2010). Apparently, neuroligins cannot compete with cerebellins at parallel-fiber synapses, possibly because cerebellins have a higher affinity for neurexins than neuroligins. Our results differ from those of Baudouin et al. (2012) in that even in analyses of constitutive NL3 KO mice using exactly the conditions of Baudouin et al. (2012), we observe no change in parallel-fiber LTD or in mGluR1/5 levels (Figures 3I, S2, S3, and S4G). We cannot currently explain this discrepancy but believe that consistent with our data, the role of cerebellins as dominant neurexin ligands in parallel-fiber synapses makes a selective contribution of NL3 as a neurexin ligand for LTD at this synapse rather unlikely.

Neuroligins have a significant role in climbing-fiber synapses as manifested by three changes in neuroligin-deficient Purkinje cells: a loss of distal climbing-fiber synapses (which account for a small percentage of the total number of synapses), a

(C–E) Climbing-fiber EPSC amplitudes are modestly decreased in NL1-KO, NL3-KO, and NL13-KO mice. Panels show representative traces (left) and summary graphs (right) of climbing-fiber synapse EPSCs in double NL13-KO (C) and single NL1-KO (D) and NL3-KO mice (E).
(F) Normal paired-pulse ratios (PPRs) of climbing-fiber synapses in Purkinje cell-specific double NL13-KO mice at P21–P25 (left, representative traces; right, summary graph).
(G) Normal parallel-fiber synapse mEPSC frequency and amplitude and in Purkinje cell-specific double NL13-KO mice (left, representative traces; right, summary graphs of the mEPSC frequency and amplitude).
(H) Normal basket/stellate cell mIPSCs in Purkinje cell-specific double NL13-KO mice (left, representative traces; right, summary graphs of the mIPSC frequency, amplitude, rise time, and decay time).
Data shown are represented as means ± SEM. Statistical inter-group comparisons were by two-tailed Student's t test, and multiple comparisons by one-way ANOVA with Bonferroni's post-test (*$p < 0.05$, ***$p < 0.001$). For additional data, see Figures S4 and S5.

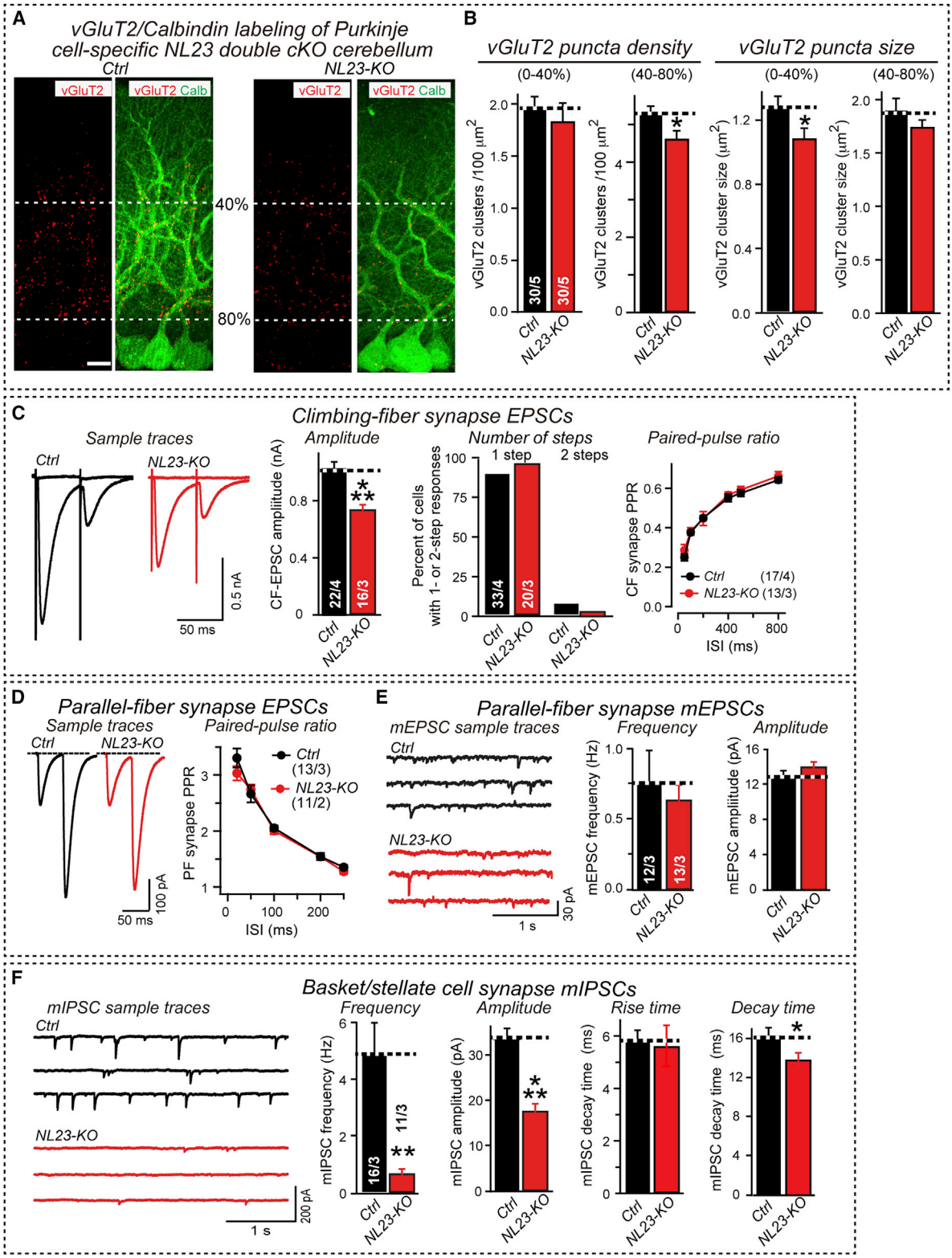

Figure 7. Impaired Climbing-Fiber and Basket/Stellate Cell Synaptic Transmission in Purkinje Cell-Specific Double NL23-KO Mice

(A) Representative confocal images of cerebellar sections from littermate control (Ctrl) and Purkinje cell-specific double NL23-KO mice. Sections were double labeled for calbindin (green, to label Purkinje cells) and vGluT2 (red, to visualize climbing-fiber synapses; scale bar = 20 μm).

(legend continued on next page)

decrease in climbing-fiber synapse size in both proximal and distal regions, and a modest reduction in climbing-fiber synaptic strength (Figures 2 and 3). Strikingly, the loss of distal climbing-fiber synapses was not observed in double NL13-KO mice, which nevertheless exhibited the same decrease in climbing-fiber synapse size and synaptic strength as triple NL123-KO mice (Figure 6). Thus, the loss of distal climbing-fiber synapses is independent of the change in climbing-fiber synapse size and function.

Viewed together, the following observations indicate that the distal climbing-fiber synapse loss is the combined result of the impairment of inhibitory synaptic transmission and of the loss of NL1 and NL3 from climbing-fiber synapses (which both function in that synapse as shown in Figure 6): (1) NL2 is only present at inhibitory synapses (Varoqueaux et al., 2004; see Figure S7), (2) the NL13-KO does not induce the dramatic impairment of inhibitory synaptic transmission present in the NL123-KO (Figure 4), (3) the NL2-KO causes a major impairment in inhibitory synaptic transmission but does not by itself cause a loss of distal climbing-fiber synapses and increases climbing-fiber synaptic strength (Figure 8), and (4) climbing-fiber synapses are only lost when all three neuroligins are deleted. The importance of NL2 for distal climbing-fiber synapses was unexpected. Its mechanism of action is unclear since it is not solely due to a loss of inhibitory synaptic strength.

Finally, neuroligins have a major role in basket/stellate cell synapses. Here, the NL2 and NL3 KOs have differential effects. The single NL2-KO causes a major decrease in evoked IPSC amplitudes (~50%) and mIPSC frequency (~75%) but not mIPSC amplitude, whereas the single NL3-KO produces no phenotype (Figures 7, 8, and S5–S7). The double NL23-KO, however, caused a larger decrease in mIPSC frequency (~90%) than the single NL2-KO and dramatically reduced the mIPSC amplitude (~50%). Thus, NL2 and NL3 both contribute to basket/stellate cell synapse function, with NL2 providing the more important contribution. Moreover, the triple NL123-KO exhibits an increase in inhibitory synapse size (Figure 2), but the NL2-KO does not despite dramatically decreasing inhibitory synaptic transmission (Figure 7). Thus, the change in synapse size is not a simple compensatory increase to make up for the decrease in inhibitory synaptic transmission. Interestingly, extrasynaptic GABA receptors appear to be normally present in triple NL123-KO cerebellum even though synaptic GABA receptors are massively depleted as indicated by the decrease in mIPSC amplitude (Figure 4), suggesting that a loss of postsynaptic GABA receptors is largely responsible for the impairment of inhibitory synaptic transmission in triple NL123 KO mice. An attractive hypothesis to account for this overall phenotype is that neuroligins anchor a postsynaptic scaffold that prevents diffusion of GABA receptors out of sub-synaptic specializations and that deletion of neuroligins produces a loss of this scaffold, resulting in a depletion of postsynaptic receptors.

The summary picture that emerges from our study is that neural circuits are generally controlled by competing actions of different *trans*-synaptic ligand-receptor pairs that dictate the organization of synapses. Neurexin-based *trans*-synaptic signaling likely is a major component to the sculpting of cerebellar synapses and circuits, but other signaling mechanisms must also play a role. This conclusion is based on the observation that deletion of all neurexin ligands tested appears to allow retention of at least some synaptic function, with the role of neuroligins in inhibitory synaptic transmission (but not synapse formation) being the most pervasive. Moreover, our data may also be relevant for understanding the role of neuroligins and neurexins in ASDs. Mutations of individual neuroligins do not cause a phenotype in the present study by blocking synapse formation or changing plasticity, but by incremental shifts in synaptic function that are commensurate with the selective impairments in mental operations observed in individuals with ASDs.

Outlook

Overall, our results raise multiple new questions. First, our data suggest that the functions of NL1 and NL3 in an excitatory synapse can be occluded by presynaptic expression of cerebellins as a competing neurexin ligand. Among others, this suggestion provides an explanation of why cerebellins are produced presynaptically, which confers synapse specificity onto their action since postsynaptic cerebellin synthesis would affect all synapses on a neuron. It raises the question, however, whether similar competitive situations between multiple ligands for a particular synaptic cell-adhesion molecule, such as neurexins, exist in other types of synapses.

Second, although the presence of cerebellins in parallel-fiber synapses likely accounts for a lack of essential function in that synapse, why does deletion of all neuroligins from Purkinje cells only modestly impair climbing-fiber synapses? We hypothesize that other neurexin ligands may contribute, and moreover that other presynaptic cell-adhesion molecules may be redundant with neurexin-based complexes (Ko et al., 2009b, 2011; Siddiqui et al., 2010; Soler-Llavina et al., 2011). If so, why are synaptic mechanisms functionally redundant, at least partially, in some synapses (e.g., climbing-fiber synapses) but not in other synapses (e.g., basket/stellate cell synapses)?

Third, how do neuroligins work mechanistically—what are the protein-protein interactions beyond neurexin-binding that mediate their effects on synapses? Although it is well established

(B) Double NL23-KO only marginally impairs climbing-fiber synapse density (left) and size (right) as assessed by vGluT2 staining.
(C) Double NL23-KO significantly decreases climbing-fiber synapse EPSC amplitudes but does not alter climbing-fiber synapse elimination or PPR (left, representative traces; left center, summary graph of the EPSC amplitude; right center, summary graph of EPSC steps to assess synapse elimination; right, PPR).
(D) Double NL23-KO has no effect on parallel-fiber synapse PPR (left, representative traces; right, summary graph).
(E) Double NL23-KO does not alter parallel-fiber synapse mEPSC amplitude and frequency (left, representative traces; right, summary graphs).
(F) Double NL23-KO massively impairs stellate/basket-cell mIPSC frequency and amplitude (left, representative traces; right, summary graphs of the mIPSC frequency, amplitude, rise time, and decay time).
All data are represented as means ± SEM; numbers of neurons/mice analyzed are shown in the bars or plots. Inter-group comparisons were done by two-tailed Student's t test; multiple comparisons were analyzed with one-way ANOVA with Bonferroni's post-test (*$p < 0.05$, **$p < 0.01$, and ***$p < 0.001$). For additional data, see Figure S6.

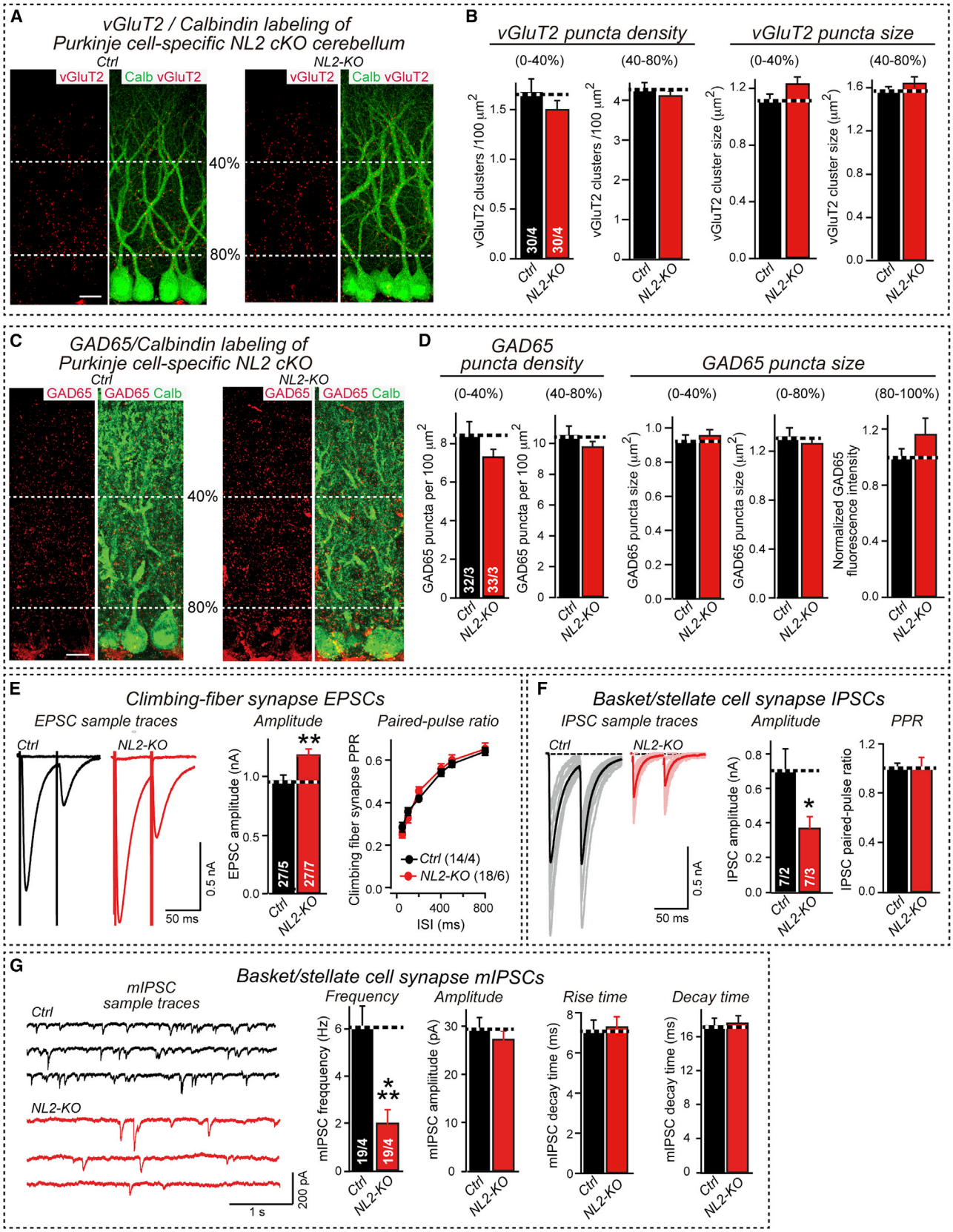

(legend on next page)

that neuroligins intracellularly bind to PDZ-domain proteins and that different sequences in their cytoplasmic tails may be functionally important (Irie et al., 1997; Iida et al., 2004; Futai et al., 2007; Shipman et al., 2011; Hoy et al., 2013; Chanda et al., 2013), very little functional information about neuroligin cytoplasmic sequences is available. In particular, no structure/function studies on neuroligins have been carried out in a physiological context without affecting endogenous microRNAs. Despite the absence of such analyses, our data as well as previous studies (e.g., Varoqueaux et al., 2006; Chubykin et al., 2007) are best consistent with a function for neuroligins as anchors for postsynaptic scaffolds that recruit receptors and other essential elements to synaptic junctions.

Finally, it is unclear how the synapse specificity of neuroligin function is determined. NL2 binds to gephyrin and collybistin (Jedlicka et al., 2011; Poulopoulos et al., 2009), but the sequences involved are present in all neuroligin isoforms, making it difficult to assess the role of this binding in specifying the inhibitory synapse function of NL2. Deciphering the molecular signals of neuroligins that guide synapse specificity remains a formidable but rewarding challenge. Thus, the understanding of neuroligins, even with the systematic and comprehensive approach chosen here, is only in its beginning, and much remains to be done.

EXPERIMENTAL PROCEDURES

Generation of Neuroligin cKO Mice, Mouse Husbandry, and Genotyping

We newly generated NL1 cKO mice and crossed them with recently generated NL2 and NL3 cKO mice (Rothwell et al., 2014; Liang et al., 2015; JAX stock number: 0023398). NL1 cKO mice were produced by Taconic (see Figure 1B). All cKO mice contain a floxed out-of-frame 5′ exon whose deletion by Cre-recombinase blocks expression of the corresponding neuroligin gene (Figure 1C) and were validated in cultured neurons. All mice were deposited in Jackson Labs for distribution.

We crossed the NL1, NL2, and NL3 cKO mice with each other and L7-Cre-recombinase transgenic mice (JAX stock number: 004146; Barski et al., 2000) to obtain homozygous NL1, NL2, NL3, NL13, NL23, and NL123 single, double, and triple cKO mice without or with the L7-Cre transgene on a hybrid C57BL/6/129Sv/CD1 background. For genotyping details, see SOMs. All procedures conformed to National Institutes of Health *Guidelines for the Care and Use of Laboratory Animals* and were approved by the Stanford University Administrative Panel on Laboratory Animal Care.

Immunohistochemistry

Immunohistochemistry experiments and other morphological studies were performed essentially as described (Rothwell et al., 2014; Tabuchi et al., 2007; see SOMs).

Gene Expression Studies Using Quantitative Immunoblotting and RT-PCR

Gene expression studies using quantitative immunoblotting and RT-PCR were performed as described previously (Tabuchi et al., 2007; Etherton et al., 2011; Aoto et al., 2013), except that all secondary antibodies for the immunoblotting measurements were labeled with fluorescent probes instead of iodinated antibodies. For details, see SOMs.

Transmission Electron Microscopy

Transmission electron microscopy was performed on Epon-embedded parasagittal sections of the cerebellum from two littermate NL123-KO and wild-type mice (P21) as described in the SOMs.

Electrophysiology

Electrophysiological experiments were carried out as described (Caillard et al., 2000; Foster and Regehr, 2004; Paukert et al., 2010; see also SOMs). Sagittal slices of the vermis (250 μm) sectioned on a vibratome (VT 1200S; Leica) were kept at 22°C–25°C in low-Ca^{2+} artificial CSF (aCSF) containing 125 mM NaCl, 2.5 mM KCl, 3 mM $MgCl_2$, 0.1 mM $CaCl_2$, 25 mM glucose, 1.25 mM NaH_2PO_4, 0.4 mM ascorbic acid, 3 mM myo-inositol, 2 mM Na-pyruvate, and 25 mM $NaHCO_3$; pH was adjusted to 7.4 by continuous carbogen gassing for >1 hr before recordings, transferred to a recording chamber, and perfused with oxygenated aCSF containing 1 mM $MgCl_2$, 2 mM $CaCl_2$ instead of 3 mM $MgCl_2$, 0.1 mM $CaCl_2$. Whole-cell recordings from Purkinje cells in cerebellar lobules IV/V (voltage clamped at −70 mV) were performed at RT with borosilicate glass pipettes (2–3 MΩ) pulled with a vertical micropipette puller (PC-10, Narishige). Focal square pulse stimuli (duration 50 μs, amplitude 0–30 V) were applied with a bipolar stimulation electrode (FHC). Climbing fibers were identified by their characteristic all-or-none response and paired-pulse depression at a 50 ms inter-stimulus interval. The number of steps of climbing-fiber EPSCs was defined as the maximal number of climbing-fiber EPSC responses with different amplitudes recorded with different stimulus strengths at different stimulation sites. Parallel fibers were stimulated in the distal molecular layer (~200 μm from the recorded Purkinje cell) and identified by their characteristic paired-pulse facilitation at 50 ms intervals. Basket/stellate cell axons were stimulated in the inner molecular layer around Purkinje cells (within 100 μm); only recordings showing an all-or-none response were accepted for further analysis (Caillard et al., 2000). For more details, see SOMs.

Statistical Analysis

Inter-group comparisons were done by two-tailed Student's t test. For multiple comparisons, data were analyzed with one-way ANOVA with Bonferroni's

Figure 8. Purkinje Cell-Specific NL2-KO Has No Effect on Inhibitory or Climbing-Fiber Synapse Numbers but Severely and Selectively Impairs Inhibitory Synapse Function

(A) Representative confocal images of cerebellar sections from littermate control (Ctrl) and Purkinje cell-specific NL2-KO mice. Sections were double labeled for vGluT2 (red, to visualize climbing-fiber synapses) and calbindin (green, to label Purkinje cells; scale bar = 20 μm).

(B) Climbing-fiber synapse density (left) and size (right), as assessed by vGluT2 staining, are not impaired by the NL2-KO.

(C) Representative confocal images of cerebellar sections double labeled with antibodies to GAD65 (red, to visualize inhibitory synapses) and calbindin (green, to identify Purkinje cells; scale bar = 20 μm).

(D) Quantifications of GAD65-immunolabelled inhibitory synapse density and size fail to reveal major changes in Purkinje cell-specific NL2 single cKO mice.

(E) NL2-KO increases climbing-fiber EPSC amplitudes by a postsynaptic mechanism (left, representative traces; right, summary graphs of the EPSC amplitude and the PPR).

(F) NL2-KO decreases evoked basket/stellate cell IPSCs (left, representative traces; right, summary graphs of the IPSC amplitude and PPR at a 50 ms inter-stimulus interval).

(G) NL2-KO strongly impairs mIPSC frequency but not amplitude (left, representative traces; right, summary graphs of mIPSC frequency, amplitude, rise time, and decay time).

All data are represented as means ± SEM; number of neurons/mice analyzed are shown in the bars or plots. Inter-group comparisons were done by two-tailed Student's t test; multiple comparisons were analyzed with one-way ANOVA with Bonferroni's post-test (*$p < 0.05$, **$p < 0.01$, and ***$p < 0.001$).

post-test; for cumulative distributions, Kolmogorov-Smirnov tests were used. Levels of significance were set as * $p < 0.05$; ** $p < 0.01$; *** $p < 0.001$. Data are shown as means ± SEM.

SUPPLEMENTAL INFORMATION

Supplemental Information includes Supplemental Experimental Procedures, eight figures, and three tables and can be found with this article online at http://dx.doi.org/10.1016/j.neuron.2015.07.020.

AUTHOR CONTRIBUTIONS

B.Z. performed the mouse genetics and electrophysiological analyses; B.Z., L.Y.C., and X.L. performed the morphological analyses; S.-J.L. performed the immunoblotting analyses; S.M. and O.G. contributed essential reagents; B.Z., L.Y.C., and T.C.S. planned the experiments, analyzed the data, and wrote the paper.

ACKNOWLEDGMENTS

This paper was supported by grants from the NIMH (R37 MH052804 to T.C.S.) and the Simons Foundation (307762 to T.C.S.), and by a fellowship from the NIMH (F32MH100745 to L.Y.C.).

Received: January 29, 2015
Revised: May 25, 2015
Accepted: July 22, 2015
Published: August 19, 2015

REFERENCES

Aoto, J., Martinelli, D.C., Malenka, R.C., Tabuchi, K., and Südhof, T.C. (2013). Presynaptic neurexin-3 alternative splicing trans-synaptically controls postsynaptic AMPA receptor trafficking. Cell *154*, 75–88.

Araç, D., Boucard, A.A., Ozkan, E., Strop, P., Newell, E., Südhof, T.C., and Brunger, A.T. (2007). Structures of neuroligin-1 and the neuroligin-1/neurexin-1 beta complex reveal specific protein-protein and protein-Ca^{2+} interactions. Neuron *56*, 992–1003.

Barski, J.J., Dethleffsen, K., and Meyer, M. (2000). Cre recombinase expression in cerebellar Purkinje cells. Genesis *28*, 93–98.

Baudouin, S.J., Gaudias, J., Gerharz, S., Hatstatt, L., Zhou, K., Punnakkal, P., Tanaka, K.F., Spooren, W., Hen, R., De Zeeuw, C.I., et al. (2012). Shared synaptic pathophysiology in syndromic and nonsyndromic rodent models of autism. Science *338*, 128–132.

Blundell, J., Blaiss, C.A., Etherton, M.R., Espinosa, F., Tabuchi, K., Walz, C., Bolliger, M.F., Südhof, T.C., and Powell, C.M. (2010). Neuroligin-1 deletion results in impaired spatial memory and increased repetitive behavior. J. Neurosci. *30*, 2115–2129.

Bolliger, M.F., Pei, J., Maxeiner, S., Boucard, A.A., Grishin, N.V., and Südhof, T.C. (2008). Unusually rapid evolution of Neuroligin-4 in mice. Proc. Natl. Acad. Sci. USA *105*, 6421–6426.

Boucard, A.A., Chubykin, A.A., Comoletti, D., Taylor, P., and Südhof, T.C. (2005). A splice code for trans-synaptic cell adhesion mediated by binding of neuroligin 1 to α- and β-neurexins. Neuron *48*, 229–236.

Budreck, E.C., and Scheiffele, P. (2007). Neuroligin-3 is a neuronal adhesion protein at GABAergic and glutamatergic synapses. Eur. J. Neurosci. *26*, 1738–1748.

Caillard, O., Moreno, H., Schwaller, B., Llano, I., Celio, M.R., and Marty, A. (2000). Role of the calcium-binding protein parvalbumin in short-term synaptic plasticity. Proc. Natl. Acad. Sci. USA *97*, 13372–13377.

Chanda, S., Marro, S., Wernig, M., and Südhof, T.C. (2013). Neurons generated by direct conversion of fibroblasts reproduce synaptic phenotype caused by autism-associated neuroligin-3 mutation. Proc. Natl. Acad. Sci. USA *110*, 16622–16627.

Chen, X., Liu, H., Shim, A.H., Focia, P.J., and He, X. (2008). Structural basis for synaptic adhesion mediated by neuroligin-neurexin interactions. Nat. Struct. Mol. Biol. *15*, 50–56.

Chen, J., Yu, S., Fu, Y., and Li, X. (2014). Synaptic proteins and receptors defects in autism spectrum disorders. Front. Cell. Neurosci. *8*, 276.

Chih, B., Engelman, H., and Scheiffele, P. (2005). Control of excitatory and inhibitory synapse formation by neuroligins. Science *307*, 1324–1328.

Chih, B., Gollan, L., and Scheiffele, P. (2006). Alternative splicing controls selective trans-synaptic interactions of the neuroligin-neurexin complex. Neuron *51*, 171–178.

Chubykin, A.A., Atasoy, D., Etherton, M.R., Brose, N., Kavalali, E.T., Gibson, J.R., and Südhof, T.C. (2007). Activity-dependent validation of excitatory versus inhibitory synapses by neuroligin-1 versus neuroligin-2. Neuron *54*, 919–931.

Comoletti, D., Flynn, R.E., Boucard, A.A., Demeler, B., Schirf, V., Shi, J., Jennings, L.L., Newlin, H.R., Südhof, T.C., and Taylor, P. (2006). Gene selection, alternative splicing, and post-translational processing regulate neuroligin selectivity for beta-neurexins. Biochemistry *45*, 12816–12827.

Etherton, M., Földy, C., Sharma, M., Tabuchi, K., Liu, X., Shamloo, M., Malenka, R.C., and Südhof, T.C. (2011). Autism-linked neuroligin-3 R451C mutation differentially alters hippocampal and cortical synaptic function. Proc. Natl. Acad. Sci. USA *108*, 13764–13769.

Fabrichny, I.P., Leone, P., Sulzenbacher, G., Comoletti, D., Miller, M.T., Taylor, P., Bourne, Y., and Marchot, P. (2007). Structural analysis of the synaptic protein neuroligin and its beta-neurexin complex: determinants for folding and cell adhesion. Neuron *56*, 979–991.

Földy, C., Malenka, R.C., and Südhof, T.C. (2013). Autism-associated neuroligin-3 mutations commonly disrupt tonic endocannabinoid signaling. Neuron *78*, 498–509.

Foster, K.A., and Regehr, W.G. (2004). Variance-mean analysis in the presence of a rapid antagonist indicates vesicle depletion underlies depression at the climbing fiber synapse. Neuron *43*, 119–131.

Futai, K., Kim, M.J., Hashikawa, T., Scheiffele, P., Sheng, M., and Hayashi, Y. (2007). Retrograde modulation of presynaptic release probability through signaling mediated by PSD-95-neuroligin. Nat. Neurosci. *10*, 186–195.

Gibson, J.R., Huber, K.M., and Südhof, T.C. (2009). Neuroligin-2 deletion selectively decreases inhibitory synaptic transmission originating from fast-spiking but not from somatostatin-positive interneurons. J. Neurosci. *29*, 13883–13897.

Hirai, H., Pang, Z., Bao, D., Miyazaki, T., Li, L., Miura, E., Parris, J., Rong, Y., Watanabe, M., Yuzaki, M., and Morgan, J.I. (2005). Cbln1 is essential for synaptic integrity and plasticity in the cerebellum. Nat. Neurosci. *8*, 1534–1541.

Hoon, M., Soykan, T., Falkenburger, B., Hammer, M., Patrizi, A., Schmidt, K.F., Sassoè-Pognetto, M., Löwel, S., Moser, T., Taschenberger, H., et al. (2011). Neuroligin-4 is localized to glycinergic postsynapses and regulates inhibition in the retina. Proc. Natl. Acad. Sci. USA *108*, 3053–3058.

Hoy, J.L., Haeger, P.A., Constable, J.R., Arias, R.J., McCallum, R., Kyweriga, M., Davis, L., Schnell, E., Wehr, M., Castillo, P.E., and Washbourne, P. (2013). Neuroligin1 drives synaptic and behavioral maturation through intracellular interactions. J. Neurosci. *33*, 9364–9384.

Ichtchenko, K., Hata, Y., Nguyen, T., Ullrich, B., Missler, M., Moomaw, C., and Südhof, T.C. (1995). Neuroligin 1: a splice site-specific ligand for beta-neurexins. Cell *81*, 435–443.

Ichtchenko, K., Nguyen, T., and Südhof, T.C. (1996). Structures, alternative splicing, and neurexin binding of multiple neuroligins. J. Biol. Chem. *271*, 2676–2682.

Iida, J., Hirabayashi, S., Sato, Y., and Hata, Y. (2004). Synaptic scaffolding molecule is involved in the synaptic clustering of neuroligin. Mol. Cell. Neurosci. *27*, 497–508.

Irie, M., Hata, Y., Takeuchi, M., Ichtchenko, K., Toyoda, A., Hirao, K., Takai, Y., Rosahl, T.W., and Südhof, T.C. (1997). Binding of neuroligins to PSD-95. Science *277*, 1511–1515.

Ito, M. (2002). The molecular organization of cerebellar long-term depression. Nat. Rev. Neurosci. *3*, 896–902.

Jamain, S., Quach, H., Betancur, C., Råstam, M., Colineaux, C., Gillberg, I.C., Soderstrom, H., Giros, B., Leboyer, M., Gillberg, C., and Bourgeron, T.; Paris Autism Research International Sibpair Study (2003). Mutations of the X-linked genes encoding neuroligins NLGN3 and NLGN4 are associated with autism. Nat. Genet. *34*, 27–29.

Jamain, S., Radyushkin, K., Hammerschmidt, K., Granon, S., Boretius, S., Varoqueaux, F., Ramanantsoa, N., Gallego, J., Ronnenberg, A., Winter, D., et al. (2008). Reduced social interaction and ultrasonic communication in a mouse model of monogenic heritable autism. Proc. Natl. Acad. Sci. USA *105*, 1710–1715.

Jedlicka, P., Hoon, M., Papadopoulos, T., Vlachos, A., Winkels, R., Poulopoulos, A., Betz, H., Deller, T., Brose, N., Varoqueaux, F., and Schwarzacher, S.W. (2011). Increased dentate gyrus excitability in neuroligin-2-deficient mice in vivo. Cereb. Cortex *21*, 357–367.

Jedlicka, P., Vnencak, M., Krueger, D.D., Jungenitz, T., Brose, N., and Schwarzacher, S.W. (2013). Neuroligin-1 regulates excitatory synaptic transmission, LTP and EPSP-spike coupling in the dentate gyrus in vivo. Brain Struct. Funct. *220*, 47–58.

Kim, J., Jung, S.Y., Lee, Y.K., Park, S., Choi, J.S., Lee, C.J., Kim, H.S., Choi, Y.B., Scheiffele, P., Bailey, C.H., et al. (2008). Neuroligin-1 is required for normal expression of LTP and associative fear memory in the amygdala of adult animals. Proc. Natl. Acad. Sci. USA *105*, 9087–9092.

Ko, J., Fuccillo, M.V., Malenka, R.C., and Südhof, T.C. (2009a). LRRTM2 functions as a neurexin ligand in promoting excitatory synapse formation. Neuron *64*, 791–798.

Ko, J., Zhang, C., Arac, D., Boucard, A.A., Brunger, A.T., and Südhof, T.C. (2009b). Neuroligin-1 performs neurexin-dependent and neurexin-independent functions in synapse validation. EMBO J. *28*, 3244–3255.

Ko, J., Soler-Llavina, G.J., Fuccillo, M.V., Malenka, R.C., and Südhof, T.C. (2011). Neuroligins/LRRTMs prevent activity- and Ca2+/calmodulin-dependent synapse elimination in cultured neurons. J. Cell Biol. *194*, 323–334.

Kwon, H.B., Kozorovitskiy, Y., Oh, W.J., Peixoto, R.T., Akhtar, N., Saulnier, J.L., Gu, C., and Sabatini, B.L. (2012). Neuroligin-1-dependent competition regulates cortical synaptogenesis and synapse number. Nat. Neurosci. *15*, 1667–1674.

Laumonnier, F., Bonnet-Brilhault, F., Gomot, M., Blanc, R., David, A., Moizard, M.P., Raynaud, M., Ronce, N., Lemonnier, E., Calvas, P., et al. (2004). X-linked mental retardation and autism are associated with a mutation in the NLGN4 gene, a member of the neuroligin family. Am. J. Hum. Genet. *74*, 552–557.

Lee, K., Kim, Y., Lee, S.J., Qiang, Y., Lee, D., Lee, H.W., Kim, H., Je, H.S., Südhof, T.C., and Ko, J. (2013). MDGAs interact selectively with neuroligin-2 but not other neuroligins to regulate inhibitory synapse development. Proc. Natl. Acad. Sci. USA *110*, 336–341.

Liang, J., Xu, W., Hsu, Y.T., Yee, A.X., Chen, L., and Südhof, T.C. (2015). Conditional neuroligin-2 knockout in adult medial prefrontal cortex links chronic changes in synaptic inhibition to cognitive impairments. Mol. Psychiatry *20*, 850–859.

Lorenzetto, E., Caselli, L., Feng, G., Yuan, W., Nerbonne, J.M., Sanes, J.R., and Buffelli, M. (2009). Genetic perturbation of postsynaptic activity regulates synapse elimination in developing cerebellum. Proc. Natl. Acad. Sci. USA *106*, 16475–16480.

Matsuda, K., Miura, E., Miyazaki, T., Kakegawa, W., Emi, K., Narumi, S., Fukazawa, Y., Ito-Ishida, A., Kondo, T., Shigemoto, R., et al. (2010). Cbln1 is a ligand for an orphan glutamate receptor delta2, a bidirectional synapse organizer. Science *328*, 363–368.

Nguyen, T., and Südhof, T.C. (1997). Binding properties of neuroligin 1 and neurexin 1beta reveal function as heterophilic cell adhesion molecules. J. Biol. Chem. *272*, 26032–26039.

Paukert, M., Huang, Y.H., Tanaka, K., Rothstein, J.D., and Bergles, D.E. (2010). Zones of enhanced glutamate release from climbing fibers in the mammalian cerebellum. J. Neurosci. *30*, 7290–7299.

Pettem, K.L., Yokomaku, D., Takahashi, H., Ge, Y., and Craig, A.M. (2013). Interaction between autism-linked MDGAs and neuroligins suppresses inhibitory synapse development. J. Cell Biol. *200*, 321–336.

Poulopoulos, A., Aramuni, G., Meyer, G., Soykan, T., Hoon, M., Papadopoulos, T., Zhang, M., Paarmann, I., Fuchs, C., Harvey, K., et al. (2009). Neuroligin 2 drives postsynaptic assembly at perisomatic inhibitory synapses through gephyrin and collybistin. Neuron *63*, 628–642.

Poulopoulos, A., Soykan, T., Tuffy, L.P., Hammer, M., Varoqueaux, F., and Brose, N. (2012). Homodimerization and isoform-specific heterodimerization of neuroligins. Biochem. J. *446*, 321–330.

Rothwell, P.E., Fuccillo, M.V., Maxeiner, S., Hayton, S.J., Gokce, O., Lim, B.K., Fowler, S.C., Malenka, R.C., and Südhof, T.C. (2014). Autism-associated neuroligin-3 mutations commonly impair striatal circuits to boost repetitive behaviors. Cell *158*, 198–212.

Sara, Y., Biederer, T., Atasoy, D., Chubykin, A., Mozhayeva, M.G., Südhof, T.C., and Kavalali, E.T. (2005). Selective capability of SynCAM and neuroligin for functional synapse assembly. J. Neurosci. *25*, 260–270.

Shipman, S.L., and Nicoll, R.A. (2012). A subtype-specific function for the extracellular domain of neuroligin 1 in hippocampal LTP. Neuron *76*, 309–316.

Shipman, S.L., Schnell, E., Hirai, T., Chen, B.S., Roche, K.W., and Nicoll, R.A. (2011). Functional dependence of neuroligin on a new non-PDZ intracellular domain. Nat. Neurosci. *14*, 718–726.

Siddiqui, T.J., Pancaroglu, R., Kang, Y., Rooyakkers, A., and Craig, A.M. (2010). LRRTMs and neuroligins bind neurexins with a differential code to cooperate in glutamate synapse development. J. Neurosci. *30*, 7495–7506.

Soler-Llavina, G.J., Fuccillo, M.V., Ko, J., Südhof, T.C., and Malenka, R.C. (2011). The neurexin ligands, neuroligins and leucine-rich repeat transmembrane proteins, perform convergent and divergent synaptic functions in vivo. Proc. Natl. Acad. Sci. USA *108*, 16502–16509.

Song, J.Y., Ichtchenko, K., Südhof, T.C., and Brose, N. (1999). Neuroligin 1 is a postsynaptic cell-adhesion molecule of excitatory synapses. Proc. Natl. Acad. Sci. USA *96*, 1100–1105.

Spruston, N., Jaffe, D.B., and Johnston, D. (1994). Dendritic attenuation of synaptic potentials and currents: the role of passive membrane properties. Trends Neurosci. *17*, 161–166.

Südhof, T.C. (2008). Neuroligins and neurexins link synaptic function to cognitive disease. Nature *455*, 903–911.

Tabuchi, K., Blundell, J., Etherton, M.R., Hammer, R.E., Liu, X., Powell, C.M., and Südhof, T.C. (2007). A neuroligin-3 mutation implicated in autism increases inhibitory synaptic transmission in mice. Science *318*, 71–76.

Takács, V.T., Freund, T.F., and Nyiri, G. (2013). Neuroligin 2 is expressed in synapses established by cholinergic cells in the mouse brain. PLoS ONE *8*, e72450.

Uemura, T., Lee, S.J., Yasumura, M., Takeuchi, T., Yoshida, T., Ra, M., Taguchi, R., Sakimura, K., and Mishina, M. (2010). Trans-synaptic interaction of GluRdelta2 and Neurexin through Cbln1 mediates synapse formation in the cerebellum. Cell *141*, 1068–1079.

Varoqueaux, F., Jamain, S., and Brose, N. (2004). Neuroligin 2 is exclusively localized to inhibitory synapses. Eur. J. Cell Biol. *83*, 449–456.

Varoqueaux, F., Aramuni, G., Rawson, R.L., Mohrmann, R., Missler, M., Gottmann, K., Zhang, W., Südhof, T.C., and Brose, N. (2006). Neuroligins determine synapse maturation and function. Neuron *51*, 741–754.

Wang, S.S., Kloth, A.D., and Badura, A. (2014). The cerebellum, sensitive periods, and autism. Neuron *83*, 518–532.

Xu-Friedman, M.A., and Regehr, W.G. (2000). Probing fundamental aspects of synaptic transmission with strontium. J. Neurosci. *20*, 4414–4422.

Yan, J., Oliveira, G., Coutinho, A., Yang, C., Feng, J., Katz, C., Sram, J., Bockholt, A., Jones, I.R., Craddock, N., et al. (2005). Analysis of the neuroligin 3 and 4 genes in autism and other neuropsychiatric patients. Mol. Psychiatry *10*, 329–332.

Zhang, C., Milunsky, J.M., Newton, S., Ko, J., Zhao, G., Maher, T.A., Tager-Flusberg, H., Bolliger, M.F., Carter, A.S., Boucard, A.A., et al. (2009). A neuroligin-4 missense mutation associated with autism impairs neuroligin-4 folding and endoplasmic reticulum export. J. Neurosci. *29*, 10843–10854.